

## Base isolation fibre-reinforced composite bearings using recycled rubber

Sengsri, Pasakorn; Marsico, Maria Rosaria; Kaewunruen, Sakdirat

DOI:

[10.1088/1757-899X/603/2/022060](https://doi.org/10.1088/1757-899X/603/2/022060)

[10.1088/1757-899x/603/2/022060](https://doi.org/10.1088/1757-899x/603/2/022060)

License:

Creative Commons: Attribution (CC BY)

*Document Version*

Publisher's PDF, also known as Version of record

*Citation for published version (Harvard):*

Sengsri, P, Marsico, MR & Kaewunruen, S 2019, 'Base isolation fibre-reinforced composite bearings using recycled rubber', *IOP Conference Series: Materials Science and Engineering*, vol. 603.

<https://doi.org/10.1088/1757-899X/603/2/022060>, <https://doi.org/10.1088/1757-899x/603/2/022060>

[Link to publication on Research at Birmingham portal](#)

### General rights

Unless a licence is specified above, all rights (including copyright and moral rights) in this document are retained by the authors and/or the copyright holders. The express permission of the copyright holder must be obtained for any use of this material other than for purposes permitted by law.

- Users may freely distribute the URL that is used to identify this publication.
- Users may download and/or print one copy of the publication from the University of Birmingham research portal for the purpose of private study or non-commercial research.
- User may use extracts from the document in line with the concept of 'fair dealing' under the Copyright, Designs and Patents Act 1988 (?)
- Users may not further distribute the material nor use it for the purposes of commercial gain.

Where a licence is displayed above, please note the terms and conditions of the licence govern your use of this document.

When citing, please reference the published version.

### Take down policy

While the University of Birmingham exercises care and attention in making items available there are rare occasions when an item has been uploaded in error or has been deemed to be commercially or otherwise sensitive.

If you believe that this is the case for this document, please contact [UBIRA@lists.bham.ac.uk](mailto:UBIRA@lists.bham.ac.uk) providing details and we will remove access to the work immediately and investigate.

PAPER • OPEN ACCESS

## Base isolation fibre-reinforced composite bearings using recycled rubber

To cite this article: Pasakorn Sengsri *et al* 2019 *IOP Conf. Ser.: Mater. Sci. Eng.* **603** 022060

View the [article online](#) for updates and enhancements.

# Base isolation fibre-reinforced composite bearings using recycled rubber

Pasakorn Sengsri<sup>1, 2</sup>, Maria Rosaria Marsico<sup>3</sup>, Sakdirat Kaewunruen<sup>1, 2</sup>

<sup>1</sup>Department of Civil Engineering, School of Engineering, University of Birmingham, Birmingham B15 2TT, United Kingdom

<sup>2</sup>Birmingham Centre for Railway Research and Education, School of Engineering, University of Birmingham, Birmingham B15 2TT, United Kingdom

<sup>3</sup>College of Engineering, Mathematics and Physical Sciences, University of Exeter, Exeter EX4 4QF, United Kingdom

pxs905@student.bham.ac.uk

**Abstract.** In the past few years, there have been a number of previous researches on the rubber isolators for resisting earthquakes. A typical bearing consists of natural rubber sheets and bonded to steel plates. For an application of using rubber bearings, numerous isolated buildings have been constructed to resist an earthquake across the countries which experience earthquakes over decades. Another application might be used in the bridge structures of railways and highways, in order to suppress vibrations and dynamic actions. The key idea is to use rubber isolators attached beneath the superstructures for attenuating the damage potential of seismic responses. This means that the rubber provides the isolators flexible in the horizontal direction and the steel makes them strong in the vertical direction. Anyways, most bearings are made of natural rubber or synthetic compound. These materials are costly and cannot be durable over time. This paper aims to develop a new design of bearing using recycled materials and fibre reinforcement. The concept is to design two models using the finite element method (FEM) as a square and circular shape for the investigation into the static and dynamic behaviour. Through, the finite element method will be conducted to evaluate structural response and effectiveness of the novel low-cost bearing. Bearing models from the analytical method based on the theory are verified by the FEM. The overall results show that the fibre square model is less effective than the fibre circular model due to the different shape factors,  $S$ . The outcome of this project will help to enable more eco-friendly bearing materials for structural, highway and railway engineers. However, a further study of designing recycled rubber bearings with the fibre-reinforced polymer should be carried out by experimental tests. The study should be also compared with the performance between the fibre and steel bearing model, in order to verify the models created by FEA more effectively.

## 1. Introduction

Over the decades, more isolated buildings have been constructed to resist earthquakes. The common idea is to use rubber isolators under the superstructures for reducing the damage potential of the seismic response. A typical bearing consists of rubber and steel layers, while the rubber provides the isolators for flexibility in the horizontal direction, the steel makes them strong in the vertical direction. However, the weight of the steel-reinforced elastomeric bearing is heavy, costly for steel and standard rubber. Therefore, the development of a new design of bearing using recycled materials and fibre reinforcement



has been studied. The first vital concept for civil engineers to design all the engineered structures around the world should be based on the capacity of the structure more than the demand for the structure. The capacity of structures should be regularly more than the demand for the structures [1]. If engineers need to obtain the first solution, they may increase the capacity of the structure because the earthquakes are uncontrollable. Therefore, a good approach to accept the demand or limit is by focusing on the ductility of the structures for the second solution. However, the first solution requires the structures having enormous member sizes of them to increase the capacity of the structure. Also, it is not economic to use this method. Thus, the conventional design codes should be the second choice, due to the more economical solution. In the case of a minor earthquake, the conventional design codes assume that the structure remains in an elastic range. Anyway, in the case of a major earthquake, the structure passes the elastic limit. Yaming [2] states that if the structural elements have suitable ductility, the structure expresses a large displacement, does not fail, and resist a vast ground motion. Base isolation attempts to attenuate the demand rather than increase the capacity because it can attenuate the dynamic response of the structure. This leads to protection of the motions transmitted from the foundation to the superstructure. For example, a rigid structure cannot resist a ground motion because of no displacement and ground acceleration on the superstructure, whilst a flexible structure can withstand a ground motion due to some ground displacement and zero acceleration on the structure.

There are many studies on the development of seismic base isolation systems around the world. The first base isolation method was presented in 1909 by a medical doctor known as J.A. Calanterioris. The idea is based on sliding. It means that a building is built on free joints and a layer of fine sand, mica, or talc. This leads to the building moving horizontally under a ground motion. Therefore, the force shear transferred to the building would be attenuated and the structure would survive under the situation [3]. In years 1876 to 1895, the “Father of Modern Seismology” was John Milne who was a Professor of Mining Engineering in Tokyo. He recommended and improved a number of seism scopes and seismographs. Examples of prior seismic base isolation method were sliding rollers, basement, balls, etc. During the same period, John Milne was studying the base isolation system at the University of Tokyo, his first experiment was based on seismic isolation system using sliding balls with rollers attached to buildings to withstand earthquakes. The previous dimension of the balls is 10 inches and later 8 inches and 1 inch. Finally, the dimension of the balls is 0.25 inches at the end of his studies [3].

The concept of applying seismic base isolation has been considered and developed for withstanding earthquakes over the last 20 years. In 1975, in New Zealand, a lead-plug bearing was first invented. Therefore, the lead-plug bearing is similar to laminated rubber bearings, but it consists of one or more circular holes as shown in Figure 1. It is placed inside the holes which have a function to increase the damping of the elastomer isolator. Anyways, the damping ratio should be proportional to the structure response. This is because if the damping value is extremely high, the efficiency of the isolation system can be reduced. To solve this problem, the lead-plug rubber should be inserted with enough number of isolators installed underneath the basement to success the required superstructure response [3].

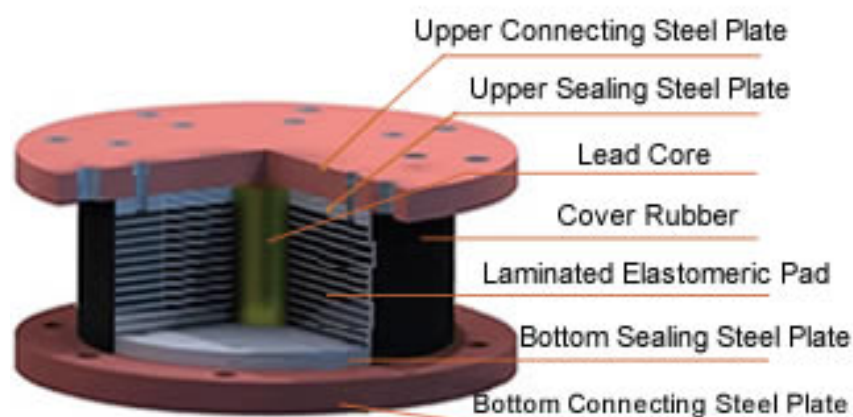


**Figure 1.** Component of elastomer isolator

A new type of elastomeric base isolation systems is using the fibre-reinforced elastomeric isolators (FREIs) to reduce the cost of the systems. In addition, the production and construction of rubber bearings for those building are more difficult than that for the fibre-reinforce isolators [4]. Also, they note that the effect of applying FREIs is the vertical pressure on the lateral response of isolators which are negligible. Anyway, the horizontal flexibility and the damping capacity are increased by decreasing the cyclic loading rate. In this paper, the analytical models based on the theory of base isolation and the numerical models from FEM will be investigated and validated to obtain static and dynamic properties. There is also a comparison of the performance between the different models in this paper.

## 2. Mechanical Characteristic of Elastomeric Bearings

Over the decades, the base isolation has been studied in the mechanical characteristic of multi-layered isolators, while applying the nonlinear method remains hard to study. Hence, the best way to obtain simple predictions is based on elastic theory. They are certified and developed by testing in the laboratory and finite element analysis, respectively.

The most important mechanical property of an isolation bearing is the horizontal stiffness, given by equation (1)

$$K_H = \frac{G \cdot A}{t_r} \quad (1)$$

As the equation (1), where  $G$  is the shear modulus of the elastomer,  $A$  is the cross-sectional area of the isolator and  $t_r$  is the total thickness of the rubber.

A significant design criterion is the vertical frequency of an isolated structure. The frequency is dominated by the vertical stiffness of the isolation system. However, the value of the vertical frequency should be much greater than the horizontal frequency. This is to protect the buckling behaviour of the isolator and rocking motion of the superstructure. The vertical stiffness of a rubber bearing is given by the formula in equation (2).

$$K_V = \frac{E_c \cdot A}{t_r} \quad (2)$$

In the above equation, where  $A$  stands for the cross-sectional area of the bearing,  $t_r$  is the total thickness of rubber, and  $E_c$  is the instantaneous compression modulus of the rubber composite under the specified level of vertical load. In addition to  $E_c$ , it is controlled by the shape factor  $S$ , as shown in the following equation (3)

$$S = \frac{\text{Loaded area}}{\text{force free area}} \quad (3)$$

Where shape factor  $S$ , is a dimensionless factor of the aspect ratio of the single layer of the rubber. For instance, a square rubber bearing having dimension  $a$  and thickness  $t$ ,

$$S = \frac{a}{4 \cdot t} \quad (4)$$

For a circular pad of diameter  $\Phi$  and thickness  $t$ ,

$$S = \frac{\Phi}{4 \cdot t} \quad (5)$$

For a square isolator, the compression modulus  $E_c$  is defined by

$$E_c = 6.73 \cdot G \cdot S^2 \quad (6)$$

For a circular pad, the compression modulus  $E_c$  is given by

$$E_c = 6 \cdot G \cdot S^2 \quad (7)$$

For critical bucking load defined above can be also simplified by

$$P_{\text{crit}} = \frac{\sqrt{2} \cdot \pi \cdot A \cdot G \cdot r \cdot S}{t_r} \quad (8)$$

Where  $r$  is the radius of gyration given by

$$r = \sqrt{\frac{I}{A}} \quad (9)$$

For a square isolator is

$$r = \frac{a}{2\sqrt{3}} \quad (10)$$

For a circular isolator is

$$r = \frac{\phi}{4} \quad (11)$$

### 3. Analytical and finite element modelling

#### 3.1 Analytical modelling

The analytical models were formed in a square and circular shape. The dimensions of both models are based on Soleimanloo and Barkhordari's research [5]. Table 1 indicates the dimension of parameters of a square and circular elastomeric bearing.

**Table 1.** Dimensions for modelling a square and circular analytical model.

Parameter	Square bearing model	Circular bearing model
Width or diameter, $a$ or $\phi$ (mm)	120.00	135.41
Thickness of rubber, $t$ (mm)	5.00	5.00
Number of rubber layer, $N_r$	8.00	8.00
Total thickness of rubber layer, $t_r$ (mm)	40.00	40.00
Thickness of fibre sheet, $t_f$ (mm)	0.5	0.5
Number of fibre sheet, $N_f$	7.00	7.00
Shape factor, $S$	6.00	6.77
Radius of gyration, $r$ (mm <sup>2</sup> )	34.64	33.85
Area of a bearing, $A$ (mm <sup>2</sup> )	14400.00	14400.00
Height of a bearing, $h$ (mm)	43.50	43.50

#### 3.2 Finite element modelling

The square and circular models (3D) were built by using Abaqus [6]. The models are dependent on many basic tutorials in Abaqus/CAE User's Guide. The tutorials for using this program are useful to build and analyse the models. Figure 2 (a) and (b) demonstrate that the mesh of the bearing model in a square and circular shape was built, respectively and also, illustrating the arrangement of fibre and rubber layers inside the models. The yellow layers are fibre and the black layers are rubber. The dimensions of these models were based on Table 1. This leads to analysing and comparing the calculations between the analytical and finite element modelling.

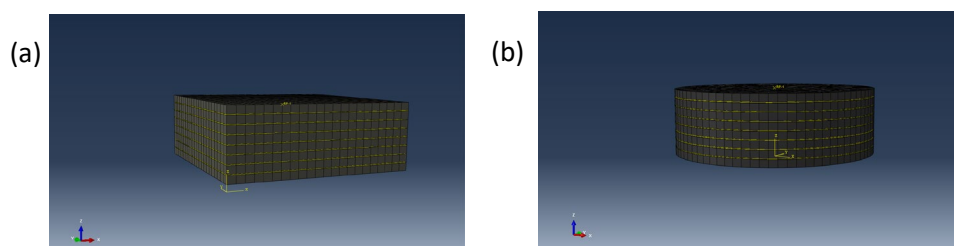


**Figure 2.** Bearing model a) square, b) circular

The layers of fibre were produced as a linear elastic orthotropic material with Young's modulus, Poisson's ratio  $\nu$ , and shear modulus,  $G$  in three dimensions, as given in Table 2. The fibre material modelled in Abaqus [6] is supposed as an orthotropic layer and the fibre layers have the same thickness of 0.5 mm. According to Mordini and Strauss [7], 'Orthotropic material have the same behaviour in both directions (related to the direction of fibre string) and different behaviour in thickness direction'. The values of parameters defined by Soleimanloo and Barkhordari [5]. They are for the behaviour of orthotropic layers. In addition, the arrangement of fibre carbon layers was discretized using a single layer of 8-node continuum brick elements with hybrid formulation (C3D8H). Table 3 shows the three different material parameters of recycled rubber.

**Table 2.** Properties of fibre material [5]

MATERIAL	E1 (N/mm <sup>2</sup> )	E2 (N/mm <sup>2</sup> )	E3 (N/mm <sup>2</sup> )	G12 (N/mm <sup>2</sup> )	G13 (N/mm <sup>2</sup> )	G23 (N/mm <sup>2</sup> )	$\nu_{12}$	$\nu_{13}$	$\nu_{23}$
Carbon Fibre (T-300, PAN)	243600	243600	10260	18200	4220	4220	0.3	0.25	0.25

Where, E: elastic modulus in three dimensions, G: shear modulus in three dimensions and  $\nu$ : Poisson's ratio in three dimensions.

**Table 3.** Different material properties of recycled rubber [8, 9]

Recycled Rubber Type (mm)	Shear Modulus, G (N/mm <sup>2</sup> )	Bulk Modulus, K (N/mm <sup>2</sup> )	Strength, E (N/mm <sup>2</sup> )	Compression Modulus, E <sub>c</sub> (N/mm <sup>2</sup> ) at strain, $\epsilon_c$ 0.1	Damping Type
SREI 150 x 150	0.37	2000	42.2	25	low
L-STP 200 x 180	1.00	2000	8.5	55	high
M-STP 200 x 190	1.83	2000	9.7	50	high

### 3.3 Static analysis

Eigenvalue Buckling Analysis, EBA provides the values of buckling load as the modes that a user requires. In this paper, the buckling modes were found in 8 modes because it is enough to determine the first positive buckling mode (compressive buckling mode) [10]. For this investigation, a vertical load, 1 N, was applied to a centre reference point on the top surface of the bearing model, because the load can distribute throughout the surface. Also, the point can move free in the horizontal and vertical direction, but the z-axial rotation is fixed. This is because it makes the model move in those directions. The end surface of the isolator models is fixed for stability while analysing. A step function is applied for the buckling analysis in Abaqus. The coefficient value of  $K$ ,  $C_{10}$ , and  $D_1$  were taken into Neo-Hooke's strain energy potential in Abaqus [6]. Also, further analysis in this section is reducing the value of  $K$  from 2000 to 1500 N/mm<sup>2</sup> to evaluate the effect of different  $K$  values on the critical buckling load by using the FEA.

### 3.4 Dynamic analysis

This dynamic investigation was carried out to obtain a hysteresis loop curve for determining the values of horizontal stiffness,  $K$  and the values of damping,  $\zeta$  for each of the two finite element models created in Abaqus [6]. Kelly and Takhirov [11] note that a hysteresis loop curve and damping ratio can be used to estimate the horizontal stiffness. However, in this analysis, the value of  $G$  which is 0.37 N/mm<sup>2</sup> was only applied to invest for the models. Anyway, the two models assume that the energy consumed in each of the cycles is linear to the frequency and rectangular to the deflection.

For this investigation, a step produce type called 'Dynamic Implicate' in Abaqus [6] was applied with 57 and 47 increments for the square and circular model, respectively with the 1-second time period as shown in Figure 3. In order to analyse, a simulated cyclic load function was inputted into the

amplitude function in the only y-axis direction on the top of the model. The function is similar to a real earthquake as given in Figure 4.

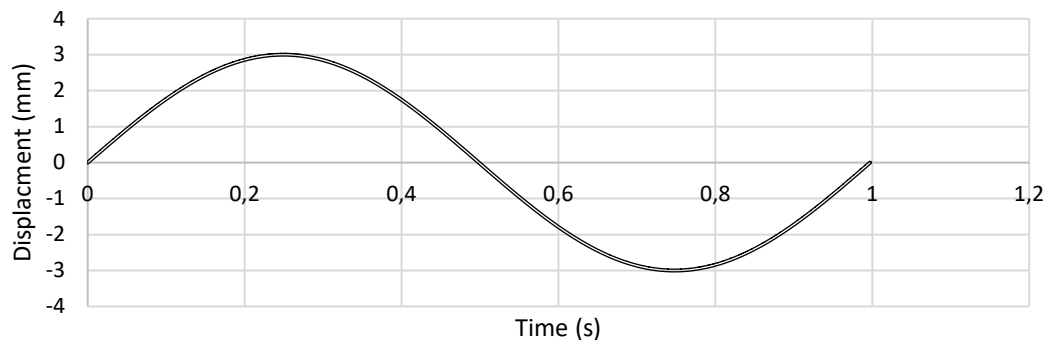


**Figure 3.** Simulated ground motion function for dynamic analysis

In addition, a vertical load to the model = 100 N similar to a weight of a simple shaking table model in a laboratory above the model and a ground motion from the cyclic load function to the top surface of the model in the horizontal direction, y-axis direction only. The boundary conditions for the top surface and the base surface are fixed and able to move in the horizontal and vertical direction, respectively. Concerning to measure the horizontal displacement, a node was set on the centre reference points on the top surface of the model. After this, a plot of correlation between shear force and horizontal deformation was carried out for each of the models. Furthermore, the values of horizontal stiffness  $K_H$  and damping ratio,  $\zeta$  can be calculated for the two models.

#### 4. Results and discussion

##### 4.1 Static analysis results

Table 4 and 5 show the vertical and the horizontal stiffness of the analytical models and the finite element analysis for the two bearing models with  $G = 0.37 \text{ N/mm}^2$  only. In the case of the square model, the values of vertical force in the linear curve are 100, 78.53, and 51.83. Also, the values of vertical deformation are 0.0102, 0.0096, and 0.0086, respectively. Therefore, the vertical stiffness of the square model is 30106.25 N/mm. Anyway, the load increment is likely to be linear as the curve graph. So, the selection of the data for estimating the vertical stiffness is valid. As the result, the differences between vertical stiffness values are slight. However, the results of vertical stiffness from the FEM is lower than that of the analytical method. This is because the non-linear curve in the first period.

**Table 4.** Comparison of the vertical stiffness of the analytical method and FEA for both models

Method	$K_v \text{ (N/mm)}$ for square, $G = 0.37 \text{ N/mm}^2$	$K_v \text{ (N/mm)}$ for circular, $G = 0.37 \text{ N/mm}^2$
Analytical	32148.28	36459.09
Finite element	30106.25	35046.67

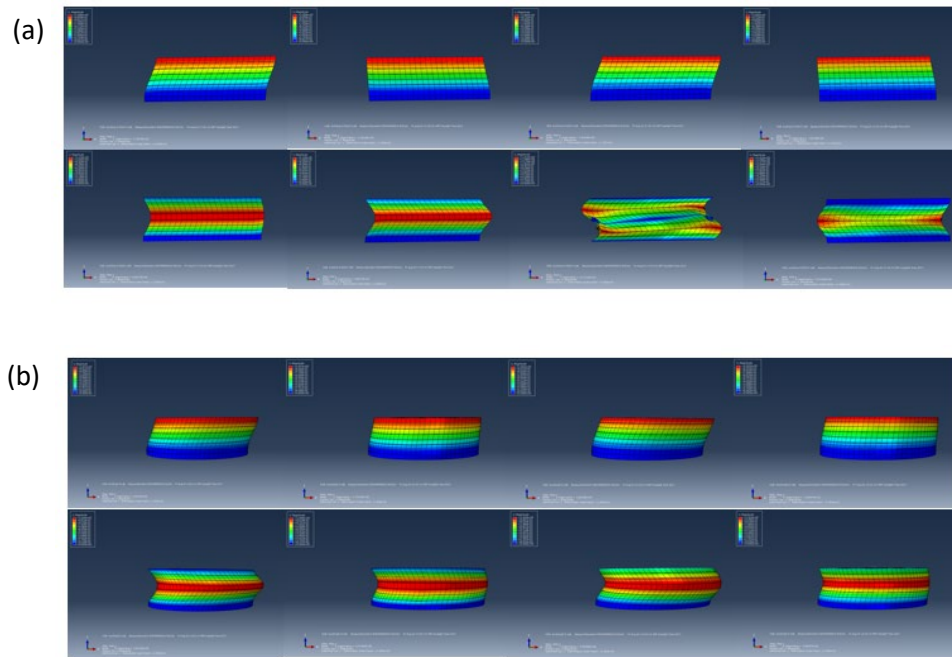
**Table 5.** Comparison of the horizontal stiffness between the analytical method and FEA for both models

Method	$K_H \text{ (N/mm}^2\text{)}$ for square, $G = 0.37 \text{ N/mm}^2$	$K_H \text{ (N/mm}^2\text{)}$ for circular, $G = 0.37 \text{ N/mm}^2$
Analytical	133.20	133.20
Finite element	125.40	125.40

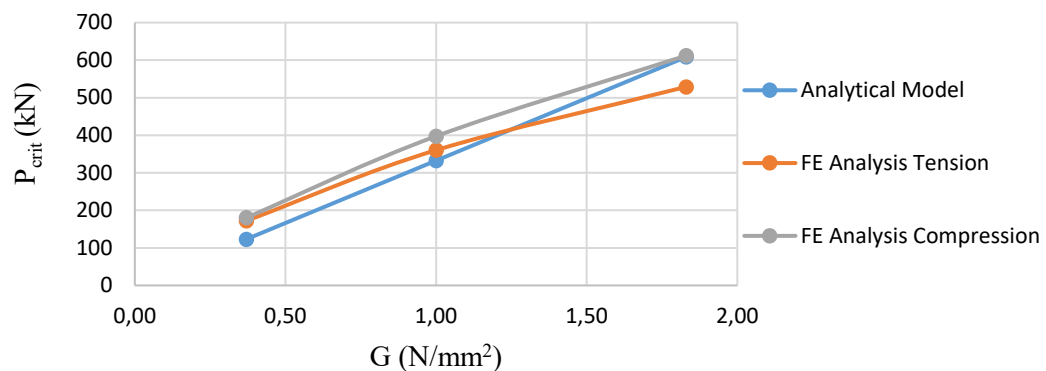


#### 4.1.1 Eigenvalue Buckling Analysis.

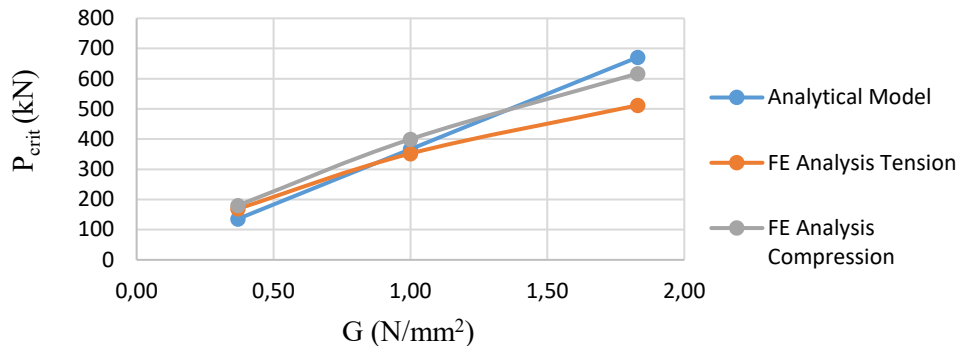
Figure 4 illustrates the 3-D views of the stress distribution of the two isolator models with shear modulus,  $G = 0.37 \text{ N/mm}^2$ . As a result, the eigenvalue buckling method provided the first 8 critical buckling modes for each of the two models. Also, the whole modes of the two models show the tension and compression loads. The tensile buckling loads for the two models are less than the compressive buckling loads [12]. However, the analytical models do not define which buckling load is tensile or compressive.



**Figure 4.** Distribution of stress contour inside the square (a) and circular (b) model for the eigenvalue buckling mode 1 to mode 8



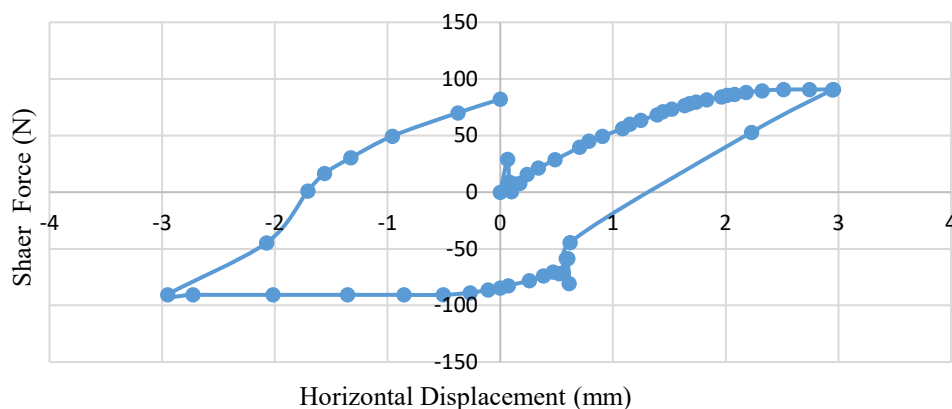
**Figure 5.** Comparison of  $P_{crit}$  and  $G$  between the FE and analytical model in a square shape



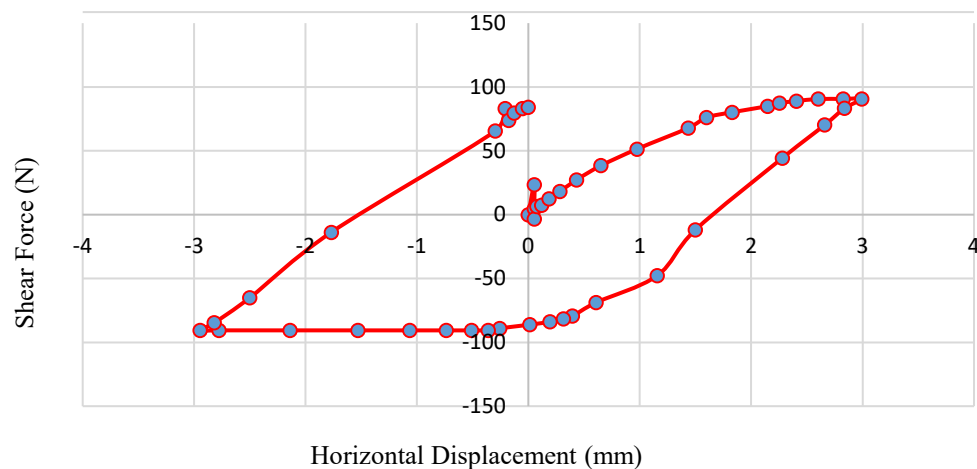
**Figure 6.** Comparison of  $P_{crit}$  and  $G$  between the FE and analytical model in a circular shape

Figure 5 and 6 indicate a comparison of the critical buckling load and the shear modulus between the FE and the analytical models in the square and circular shape, with the 3 different shear modulus ( $G = 0.37 \text{ N/mm}^2$ ,  $G = 1.00 \text{ N/mm}^2$ , and  $G = 1.83 \text{ N/mm}^2$ , respectively). It is obvious that the circular model is more effective than the square model. In addition, the critical buckling loads in compression are more than those in tension for the finite element method. Moreover, the compressive buckling loads in the circular FE model in the first part of the curve are much greater than the buckling load results from the analytical models. It is about 1.3 times more than that. For the last part of the curve, the compressive buckling loads in the FEM are much less than the buckling load results from the analytical models, approximately 0.9. However, the finite element analysis cannot provide the same values equal to the results in the analytical modelling, because the FEM is likely to consider the effect of bulk modulus that is required for the data of bulk modulus in the Neo-Hookean function for rubber material properties.

#### 4.2 Dynamic analysis results



**Figure 7.** Hysteresis loop curve of the square isolator model



**Figure 8.** Hysteresis loop curve for the circular isolator model

Figure 7 and 8 present a hysteresis loop curve of the square and circular model for the horizontal maximum displacement of the bearing models equal to 3 mm. Table 6 and 7 indicate the values of horizontal stiffness,  $K_H$  and equivalent damping ratio of the two models. It is clear that the results between the analytical models and finite element models are different, but the findings of stiffness and damping ratio for the different models are close together. This is because the analysis in Abaqus [6] for the horizontal stiffness considers the effect of fibre reinforcement. Meanwhile, the analytical models are possible to consider the effect of rubber only.

**Table 6.** Comparison of the horizontal stiffness and equivalent damping ratio of the square isolator model,  $G = 0.37 \text{ N/mm}^2$

	Horizontal stiffness, $K_H$ (N/mm)	Equivalent damping ratio, $\zeta$ (%)
Analytical model	133.20	-
Finite element model	30.70	57.77

**Table 7.** Comparison of the horizontal stiffness and equivalent damping ratio of the circular isolator model,  $G = 0.37 \text{ N/mm}^2$

	Horizontal stiffness, $K_H$ (N/mm)	Equivalent damping ratio, $\zeta$ (%)
Analytical analysis	133.20	-
Finite element model	30.53	60.35

It is confirmed that the finite element method has the potential for modelling and estimating the mechanical characteristics of the fibre-reinforced isolator models. This is because the values of  $K_H$  in the finite element analysis are lower than those in the analytical modelling. When the bearing models have a deflection, the horizontal stiffness reduces [3]. For damping ratios, they are quite high for the two models, due to the low horizontal stiffness, but the circular model has a slightly higher damping ratio. Whilst, the analytical model did not provide the damping ratio for both the models.

## 5. Conclusion

In general, there are numerous base isolation methods used for resisting earthquakes for structures of buildings or attenuating vibration for bridges of highways or railways. Convenient steel-reinforced rubber bearings are composed of rubber layers and steel plates. These materials are costly and cannot be durable over time. Therefore, new considered materials used in elastomeric isolators should be more

effective, less costly, lighter, and eco-friendlier. The current paper presents the possibility of the development of a new bearing design of using recycled materials and fibre reinforcement. The outcomes show that the finite element method (FEM) has the potential for modelling and analysing for base isolation bearings. This is because the FEM provides the distribution of stress contour, the 3D-views of critical buckling behaviour in tension and compression, hysteresis loop curves, and equivalent damping ratios. This means the FEM is a suitable method to use for analysing the models under static and dynamic loads, but the analytical method did not provide the dynamic behaviour in this paper. However, the finite element method has a use limitation of the software program to produce a bearing model. Due to the maximum nodes (20,000 nodes). It might be concluded that the verifications between the analytic and FE modelling are satisfying. Furthermore, it is clear that the circular model is more effective than the square model due to different shape factors, S and other factors. It is recommended that the determined parameters of elastomeric isolators should be used in modelling of analytical and FE method where the influences of fibre material on the base isolation will be taken into account. Also, an experiment to verify the fibre models should be carried out in a further research, in order to be used in reality.

### Acknowledgment(s)

Authors would like to thank the technical staff at University of Exeter for their kind support, in order to allow the use of Abaqus FEA and support to complete the analysis. In addition, this project is partially supported by European Commission's Shift2Rail, H2020-S2R Project No. 730849 "S-Code: Switch and Crossing Optimal Design and Evaluation".

### References

- [1] T. E. Kelly, "Base Isolation of Structures," *Holmes Consulting Group Ltd.*, 2001.
- [2] W. Yaming, Modeling, "Analysis and Comparative Study of Several," *Seismic Passive Protective Systems for Structures*, [online] 1997, Available at: <<https://scholarship.rice.edu/bitstream/handle/1911/17140/1384417.PDF?sequence=1/>>.
- [3] F. Naeim and M. Kelly, *Design of Seismic Isolated Structures*, John Wiley & Sons, Inc., Canada, 1999.
- [4] F. H. Dezfuli and M. H. Alam, *Experiment-Based Sensitivity Analysis of Scaled Carbon-Fiber-Reinforced Elastomeric Isolators in Bonded Applications*, [online] 2016, Available at: <<http://www.mdpi.com/2079-6439/4/1/4/html/>>.
- [5] H. S. Soleimanloo and A. Barkhordari, "Effect of Shape Factor and Rubber Stiffness of Fiber-reinforced Elastomeric Bearings on the Vertical Stiffness of Isolators," *Trends in Applied Sciences Research*, [online] 2013, volume 8, p.14-25, Available at: <<http://scialert.net/fulltext/?doi=tasr.2013.14.25/>>.
- [6] Abaqus/CAE User's Guide, [online], Available at: <<http://abaqus.software.polimi.it/v6.14/books/usi/default.htm/>>.
- [7] A. Mordini and A. Strauss, *An innovative earthquake isolation system using fibre reinforced rubber bearings*, [online] 2008, Available at: <[https://www.researchgate.net/publication/222650079\\_An\\_innovative\\_earthquake\\_isolation\\_system\\_using\\_fibre\\_reinforced\\_rubber\\_bearings/](https://www.researchgate.net/publication/222650079_An_innovative_earthquake_isolation_system_using_fibre_reinforced_rubber_bearings/)>.
- [8] B. Özden, *Low-Cost Seismic Base Isolation Using Scrap Tire Pads (Stp)*, [online] 2006, Available at: <<https://etd.lib.metu.edu.tr/upload/12607193/index.pdf/>>.
- [9] I. Buckle, S. Nagarajaiah and K. Ferrell, *Stability of Elastomeric Isolation Bearings: Experimental Study*, [Online] 2002, Available at: <<http://ascelibrary.org/doi/abs/10.1061/%28ASCE%290733-9445%282002%29128%3A1%283%29%29/>>.
- [10] P. Dvorak, *Buckling Analysis with FEA*, [online] 2011, Available at: <<http://www.machinedesign.com/fea-and-simulation/buckling-analysis-fea/>>.
- [11] M. J. Kelly, and M. S. Takhirov, *Analytical and Experimental Study of Fiber-Reinforced Elastomeric Isolators*, [online] 2001, Available at: <[http://peer.berkeley.edu/publications/peer\\_reports/reports\\_2001/0111.pdf/](http://peer.berkeley.edu/publications/peer_reports/reports_2001/0111.pdf/)>.
- [12] M. J. Kelly and S. M. Takhirov, Tension Buckling In Multilayer Elastomeric Isolation Bearings, *Journal of Mechanics of Materials and Structures*, [online] 2007, Available at: <<http://msp.org/jomms/2007/2-8/jomms-v2-n8-p16-s.pdf/>>.